RESEARCH ARTICLE

Dev Dynamics
DOI10.1002/dvdy.223

Embryo, larval, and juvenile staging of *Lytechinus pictus* from fertilization through sexual maturation.

Katherine T. Nesbit[1], Amro Hamdoun[1*]

[1]Marine Biology Research Division, Scripps Institution of Oceanography, University of California San Diego

9500 Gilman Drive, La Jolla CA 92093-0202 USA

*Corresponding Author (ahamdoun@ucsd.edu ; 858-822-5839)

Grant Sponsor and Numbers: NIH ES027921 and ES030318; NSF 1840844

Key Words: sea urchin, model organism, staging, larva

Received: Jan 30, 2020;Revised: Jun 17, 2020;Accepted: Jun 21, 2020

ABSTRACT:

Background: Sea urchin embryos have been used for more than a century in the study of fertilization and early development. However, several of the species used, such as *Strongylocentrotus purpuratus*, have long generation times making them suboptimal for genetic, transgenerational studies. **Results:** Here, we present an overview of the development of a rapidly developing echinoderm species, *Lytechinus pictus,* from fertilization through sexual maturation. When grown at room temperature (20°C) embryos complete the first cell cycle in 90 minutes, followed by subsequent cleavages every 45 minutes, leading to hatching at 9 hours post-fertilization (hpf). The swimming embryos gastrulate from 12-36 hpf and produce the cells which subsequently give rise to the larval skeleton and immunocytes. Larvae begin to feed at 2 days and metamorphose by 3 weeks. Juveniles reach sexual maturity at 4-6 months of age, depending on individual growth rate. **Conclusions:** This staging scheme lays a foundation for future studies in *L. pictus,* which share many of the attractive features of other urchins but have the key advantage of rapid development to sexual maturation. This is significant for multigenerational and genetic studies newly enabled by CRISPR-CAS mediated gene editing.

INTRODUCTION:

The diversity of animal form and function within the oceans provides a rich platform for biological discovery. Many marine organisms – including annelids[1], choanoflagellates[2], cnidarians[3], copepods[4], diatoms[5], echinoderms[6], oysters[7], sponges[8], and tunicates[9] among others – have been used in the lab, leading to a long history of significant contributions coming from marine organisms[10-17]. Echinoderms in general, and the sea urchin in particular, have played a foundational role in experimental embryology. Each female releases millions of eggs in a single spawning, fertilization occurs externally, eggs and embryos are large and relatively transparent, and development is rapid and synchronous in little more than a dish of sea water. In addition, mRNAs, guide RNAs, morpholinos, proteins, and small molecule reporters can be easily delivered into the egg by microinjection[6], facilitating the manipulation of developmental pathways.

The most frequently used urchin species is the purple sea urchin, *Strongylocentrotus purpuratus.* Several other species including *Lytechinus variegatus, Paracentrotus lividus*, and *Hemicentrotus pulcherrimus* are also used where they are more readily available. The genome of *S. purpuratus* was first of these to be published[18] and the resulting resource[19] has greatly contributed to the utilization of this species. However, there remain major limitations to the widely used echinoderm species in modern cell and developmental biology. Perhaps the most significant of these is their limited utility in multigenerational genetic studies, namely due to

their long generation times. In the case of *S. purpuratus* the generation time is at least 11 months[20,21], and perhaps as long as two years for robust reproduction[20], making the generation of genetic lines a difficult prospect.

Lytechinus pictus (aka the white or painted urchin) is an attractive alternative to *S. purpuratus*. These urchins share most of the advantages of other urchins but, unlike species such as *S. purpuratus, L. pictus* have relatively short generation times of 4-8 months[22,23]. In addition, they can be cultured at room temperature (20-22°C) and the adults have small body sizes (~1-4 cm test diameter). This rapid development and smaller adult size make the establishment of genetic lines (inbred and transgenic) an attainable goal.

L. pictus is native to the East Pacific Ocean, with a geographic range spanning from Central California to Cedros Island, Mexico[24]. This species is approximately 40 million years diverged from *S. purpuratus*, and >200 million years separated from sea urchins of the genus *Arabacia* and the sand dollar *Dendraster excentricus*[25-27]. *L. pictus* is an abundant urchin species and has been reported to live on sandy-bottoms and in sea grass bays, as well as in and around kelp beds at depths between 2 m - 300 m[28]. Originally thought to be a distinct species from *Lytechinus anamesus*, cross-fertilization between *L. pictus* and *L. anamesus*[29], and later molecular evidence from mitochondrial DNA and bindin[24], indicates that these are one species. In the laboratory, *L. pictus* live between 7-9 years, and grow to approximately 4 cm test diameter[23].

Prior work on culturing of *L. pictus* laid a foundation for generating a standard staging scheme for this species[22,23]. However, a gap in what is known is a detailed description of embryogenesis and larval morphogenesis useful for staging embryos. Here we provide updated and detailed imaging of a developmental staging scheme for *L. pictus* including key developmental events in embryogenesis such as early cleavage, blastula stages, gastrulation, as well as summaries of later larval development, and post-metamorphic life history. We aimed to compare our staging scheme with the timing of development in *S. purpuratus* to assist in comparability across species. This staging scheme will help standardize work across labs and help establish spatial and temporal maps of major developmental events.

RESULTS:

Early cleavage stages

L. pictus eggs (Fig. 1A) average 110 µm in diameter and form a conspicuous fertilization envelope (Fig. 1B) following the initiation of the cortical reaction at fertilization[30] and coinciding with changes in the electrical potential of the egg[31]. At 20°C, the first cell cycle takes 1.5 hours (Fig. 1C) and two subsequent symmetric cleavages (Fig. 1D, E) occur in the following 45-minute intervals (2.25 and 3 hpf). The fourth division, which forms the 16-cell embryo (Fig. 1F), occurs at 3.75 hpf and is the first asymmetric cell division, giving rise to four macromeres and four smaller micromeres in early cleavage. Division of all the cells except the micromeres occurs

next, at 4.5 hpf, yielding a 28-cell stage embryo (Fig. 1G). The fifth cleavage gives rise to four micromeres and four small micromeres. The micromeres ultimately give rise to the primary mesenchyme cells which form the larval skeleton while the small micromeres are presumed to directly or indirectly contribute to formation of the germ line[32]. Small micromeres of *L. pictus* have reduced efflux transport activity[33] which can be used to selectively load these cells with small molecule fluorescent substrates of transporters. By 5.75 hpf, the embryo is at the 60-cell stage (Fig. 1H) and at this stage, septate cell junctions are beginning to form[34], which help segregate the contents of the blastocoel from the external environment.

Expansion of the blastocoel and gastrulation

The cavity between cells of the early embryo expands quite dramatically between the fifth and tenth cleavages, and between 6.5-7.5 hpf the embryo is in the early blastula stages (Fig. 2A-B). The opening to the blastocoel is visible and a cluster of small micromeres, which have divided to a total of 8 cells, reside at the vegetal pole of the embryo (Fig. 2B, white arrow). The cavity of the blastocoel is more pronounced and changes in the morphology of the layer of cells from more rounded to an intermediate shape are apparent.

By 8 hpf the embryo is a mature blastula (Fig. 2C) with cell shapes more akin to a regularly spaced, columnar epithelium. Nuclei are slightly closer to the basolateral membrane, and the vegetal pole cluster of small micromeres becomes more difficult to resolve. The

blastulae are ciliated at this stage and spin within the envelope, eventually hatching by 9 hpf (Fig. 2D). At this stage the cells at the vegetal pole will begin to thicken, forming a mesenchyme blastula stage embryo (Fig. 2E) by 12 hpf. Signs of delamination and the ingression of a population of cells, the primary mesenchyme cells (PMCs) which give rise to skeletogenic cells[35,36] (Fig. 2F, white arrow), is evident by 15 hpf in *L. pictus*. This classic epithelial-mesenchymal transition ends the blastula phases and marks the subsequent onset of gastrulation.

Gastrulation of the embryo occurs in two main phases - primary and secondary invagination. Primary invagination is initiated following PMC ingression, when the thickened vegetal plate bends inward. This process is assisted in part by cues from bottle cells[37,38] and micromeres[39]. The majority of PMC ingression at the vegetal pole (Fig. 3A) is completed by 17 hpf. Bending of the vegetal plate characteristic of primary invagination, and the arrangement of ingressed PMCs into an ordered ring (Fig. 3B) begins at 18 hpf and is complete by 20 hpf. After primary invagination, a slight pause occurs before the pronounced elongation of the archenteron. At around 24 hpf, secondary invagination is underway and the archenteron has begun to extend through the blastocoel; secondary mesenchyme cells (SMCs), which give rise to muscle and immune cell types such as pigment cells, are evident in the blastocoel and at the tip of the archenteron at this mid-gastrula phase (Fig. 3C). The SMCs have long filopodia which are easily visible halfway through gastrulation. These filopodia extend towards the animal pole

and can interact with surrounding cells[40]. The subset of SMCs that will further differentiate into pigment cells are migrating through the blastocoel to later embed into the ectoderm. There are also distinct arrangements of PMCs into the triradiate skeleton. By late gastrulation (Fig. 3D), at 30 hpf, the archenteron has crossed the space of the blastocoel and the arrangements of skeletogenic cells are clear and they have begun to form skeletal rods branching out from the origins of the triradiate (Fig. 3D, white arrow). The primordial germ cells (PGCs) are presumed to migrate to the left and right coelomic pouches during later gastrulation and into the prism stage (Fig. 3F, white arrows).

By 38 hpf embryos are at the late prism stage (Fig. 3F) and mineralization of skeletal rods is apparent, while the archenteron has a more pronounced bend towards the oral side of the animal indicating it is nearly ready to fuse with the ectoderm to form the mouth. Compartmentalization and functional patterning of the larval gut is ongoing throughout gastrulation, though morphologically the gut is still very simple until later in development when it differentiates further into the tripartite fore-, mid-, and hindgut.

Larval development

The first larval stage of *L. pictus* is the pluteus stage (Fig. 3F) which occurs by 2 days post-fertilization (dpf). At this time the larvae have three distinct gut compartments, the esophagus, stomach, and intestine (corresponding to the former fore- mid- and hindgut)[41].

Larvae at 2 days will begin to filter feed phytoplankton such as *Rhodamonas lens* from the surrounding water. The larvae also have a population of conspicuous immunocytes termed pigment cells which contain granules of the autofluorescent pigment echinochrome (Fig. 3F, insets).

Subsequent larval development in sea urchins is divided up into stages based on the progression of key morphological features, such as the acquisition of additional pairs of arms, extension and differentiation of the left and right coeloms, formation of epaulettes and the vestibule, and elaboration of the rudiment structures[42]. Additional staging schemes detailing later larval development, focus primarily on the maturation of the rudiment with special attention to skeletal features and tissue organization of juvenile structures[43].

In *L. pictus*, the majority of larvae are at Stage I (Fig 4A-I) at 3dpf. During this stage feeding is evidenced by the red digestive remnants of *Rhodamonas* in the stomach. Between Stage I and Stage II (Fig. 4A-II), there is thickening of the tissue that eventually forms the oral hood (white arrow, Fig. 4A-II). The left and right coeloms extend along the stomach of the larva. The extension of the left and right posterodorsal arms during Stage III larvae (4A-III, yellow arrow) is apparent at 7 dpf. In *L. pictus* there is further elaboration of the oral hood and it extends to overhang the mouth. The tissue that forms the left and right preoral arms is not yet fully extended. There is mineralization of the skeletal rods that support the posterodorsal pair of arms, and evidence of invagination of the vestibule on the left side of the larva (Fig. 4A-III,

white arrow). The tissue which forms the vestibule folds inward towards the gut, where it will eventually meet the coelomic structures on the left side of the larva (Figure 4B-III, yellow dashed line).

As the posterodorsal arms continue to extend, initiation of the development of rudiment structures occurs, marking a Stage IV larva (Fig. 4A-IV, white arrow). The early rudiment appears as a crescent-shaped structure adjacent to the gut (Figure 4B-IV, yellow dashed line). Cells that originally migrated to the left coelomic pouch during embryogenesis contribute to the rudiment, which matures into the body of the juvenile animal at metamorphosis. The completion of extension of the preoral arms is evident in a Stage V larva (Fig. 4A-V, yellow arrow) which occurs between 10-12 dpf in *L. pictus*. The rudiment elaborates and organizes folds of tissue into a pentagonal disc (Fig. 4B-V, yellow dashed line) as the larva develops into Stage V (Fig. 4A-V, white arrow).

As the rudiment matures, three pedicellariae are formed which will be carried through metamorphosis (Fig. 4A-V, grey arrows). These structures persist in a Stage VI larva (Fig. 4A-VI) and precede the state known as competency at 3 weeks post-fertilization (wpf). At the final stage (Stage VII) the larva contains a mature rudiment with 5 tube feet and mineralized spines that are tucked away within the larval body. The rudiment sits adjacent to the gut, and when the larvae are ready to undergo metamorphosis the gut turns a greenish color and the tissue acquires a scaled or textured appearance. Tube feet within the rudiment will extend and

emerge from the larval body. The larvae bend the arms to the side and attach to the benthos during metamorphosis, allowing the body of the juvenile to emerge from the larva and an extensive tissue reorganization occurs[44,45] which includes shedding of skeletal rods and resorption of larval arm tissue.

Juvenile development to adulthood

At 24 hours post-metamorphosis (hpm) the newly settled juvenile (Fig. 5A) has 5 tube feet and 20 walking spines. The body of the animal typically contains a pale yellowish-green pigmented swirl, and sometimes remnants of larval tissue can be observed. This pigmented section, and the overall main body of the juvenile is freckled with red pigment cells retained from the larva. The pedicellariae from the larva are also retained. In newly metamorphosed animals, there are also 10 additional juvenile spines that are located on the aboral side. As juveniles continue to grow, they feed on diatoms and biofilms after formation of the teeth between 4-5 days post-metamorphosis (dpm). They will continue to develop additional tube feet and walking spines, the plates that form the test will start to fuse, and the structure of the anal plate becomes more apparent. By 4-months post-metamorphosis, the animal has a white to orange-ish appearance. The pigment cells that were once observed following metamorphosis are no longer visible. The animals eventually acquire a purple pigmentation at the base of the spines during their post-metamorphic growth period.

At four months, the range of body sizes for animals in our hands is between 1-15 mm in diameter, with growth rate post-metamorphosis being variable, even among siblings reared under identical conditions. Although sexual maturation appears a function of both age and size, we have been able to most reliably spawn animals that are 9-10 mm diameter, consistent with previous reports[23].

DISCUSSION:

Towards a unified echinoderm development staging scheme.

This paper provides an initial staging scheme for *L. pictus*. Knowing the precise timing of specification and differentiation of important cell populations is essential to being able to manipulate the embryo and provide a common language for discussion of development. Perhaps the most well-recognized standardized staging schemes come from *Xenopus*[46-48], zebrafish[49], and chick[50]. Each of these vertebrate models has unique advantages and improved accessibility for studying specific processes in development such as nervous system development, regeneration, or formation of limb buds. Expanding on the available standardized staging schemes to include invertebrates helps to query processes less easily accessed in vertebrates. In the case of sea urchins these include fertilization, early cell divisions and gastrulation to name a few.

There have been numerous descriptions of the morphologies of other echinoderms including members of the genera *Arabacia*[51], *Echinus*[52], and *Strongylocentrotus*[53-55]. Of these, *S. purpuratus* is arguably the species with the most detailed descriptions of early cleavages, and later larval development from feeding stages through metamorphosis[42,43]. However, many of the existing descriptions are fragmentary, and do not capture all of development through the life cycle. Thus, there is need for standardized staging schemes spanning the entire life cycle, such as the one presented here.

Here we have shown that, like other echinoderms, the early stages of development in *L. pictus* occur rapidly and synchronously. There are limited morphological differences of *L. pictus* in comparison to *S. purpuratus*, the key divergence focuses on timing of important developmental structures and processes. The first asymmetric cleavage, forming the micromeres, occurs by 3.5 hpf, small micromeres form by 5.75 hpf, and hatching happens in 9 hours. By comparison, it takes *S. purpuratus* 2-2.5 hours for the first cell division, 6.5 hours to reach the first asymmetric division forming the micromeres, and 27 hours to hatch from the fertilization envelope when cultured at 12°C [56]. Thus, experiments pertaining to early development can be completed in the course of a single day in *L. pictus*.

Progression through the larval period for *L. pictus* also occurs more rapidly and follows the progression of major events and development of core morphological structures that is observed in *S. purpuratus,* but in half the time. For example, feeding for *L. pictus* begins by 2

days, whereas feeding of *S. purpuratus* occurs at 4 days[42]. The extension of the left and right posterodorsal arms during Stage III larvae is apparent at 7 dpf. In *S. purpuratus* this stage is achieved at the earliest 18 dpf, but can take as long as 28 days[42]. The completion of extension of the preoral arms is evident in a Stage V larva between 10-12 dpf in *L. pictus*. To reach an equivalent stage in *S. purpuratus* takes 25-35 days[42]. Metamorphosis of *L. pictus* occurs at 21 days, compared to between 40-80 days in *S. purpuratus*[42,56] .

Echinoderms with similar developmental tempos include the Panamanian populations of *L. variegatus* which have generation times on the order of 6-8 months[57], comparable to *L. pictus*. *Temnopleurus reevesii* can also achieve maturity between 6-10 months[58] under optimal conditions, making its generation time similar to *L. pictus*. Those working with *Paracentrotus lividus* have started to compile similar staging schemes[59] and it may also have comparable generation times of approximately 5 months to earliest gamete production[28]. However, the prevalence of *L. pictus* on the West Coast of the United States, the optical transparency of their eggs, the ability to culture at room temperature (20°C), and the smaller adult body sizes all lend to preference for this species in our hands.

Conclusions: Historical and future contributions from research in L. pictus

There have already been a number of important contributions from *L. pictus*, most notably in the study of fertilization and early embryogenesis. For example, activation of *L. pictus*

and *S. purpuratus* eggs with ionophores, and the resulting observations of respiration and protein synthesis provided evidence that egg activation was independent of extracellular ions and dependent on the release of intracellular calcium[31,60]. The dynamics of the endoplasmic reticulum (ER) membrane at fertilization was first described in the eggs of *L. pictus*[61]. Some of the first promoters studied in sea urchins were the metal-responsive elements and regions upstream of *metallothionein* (*MT1*) in *L. pictus*[62,63]. Sea urchins, including *L. pictus*, were widely used in the early studies of mRNA translation and protein synthesis in early development[64-66]. This included the early work of Nemer and colleagues demonstrating that a diverse array of mRNAs stored in the egg of *L. pictus* encode the newly synthesized proteins of the early embryo[67]. *L. pictus* were also used in landmark studies on the cell cycle showing changes in calcium concentration during migration of the pronuclei, the breakdown of the nuclear envelope, during the transition between metaphase and anaphase, as well as during cleavage[68].

Gene editing has now become widespread in marine organisms, including sea urchins[69-73]. During this "CRISPR era"[74-76] the ability to rear juveniles, generate lines[58] and investigate later life developmental impacts resulting from early events in embryogenesis is going to be of increasing importance. The comparatively short generation time of *L. pictus* enables opportunities to create inbred lines of animals with reduced variability and stable genetic backgrounds for manipulation. The growing collection of community resources for working with *L. pictus* also make targeted molecular and genetic studies achievable. This includes a

transcriptome and fully sequenced genome that will soon be publicly available[77]. This would provide a pathway to target ubiquitous genes in specific cell types, or to study longer-term consequences of the environment through action on development. Understanding of ecological and evolutionary development of *L. pictus* could strengthen our understanding of the processes that control development across echinoderms.

EXPERIMENTAL PROCEDURES:

Culturing of Larvae

Adult animals were spawned by injection of 100-150 µL of 0.55 M KCl through the peristomal membrane. Females were inverted and kept submerged in filtered sea water (FSW) during spawning, and sperm was collected undiluted and kept at 15°C until use. Eggs were washed 6-10 times with FSW and visually examined for quality before fertilization. Eggs were fertilized using 2-3 drops of a fresh sperm dilution (2 µL semen into 40 mL FSW). Eggs were checked for fertilization success, where only batches of eggs with >98% successful fertilization were used. Embryos were grown with agitation at room temperature (20°C) as previously described[77]. Briefly, embryos were grown in FSW at a concentration of 1 embryo per mL until hatching from the fertilization envelope. Upon hatching, embryos were further diluted to a concentration of 1 embryo per 3 mL. Larvae were fed the red flagellated algae *Rhodamonas lens* starting at 2 days post-fertilization (dpf) and received water changes 3-4 times a week through gentle reverse filtration. Larval health was checked visually throughout development (more frequently during embryonic stages, and on a daily basis during larval development). Cultures with >10% of larvae displaying signs of stress or poor health (i.e. asymmetry, exposed skeletal rods, prolapse of the gut), were discarded. Healthy larvae were observed and imaged as described below. Metamorphosis was induced by a 60-minute exposure to 50 mM excess KCl in FSW, followed by 6 washes with FSW. Competent larvae were left to recover from the KCl

exposure in culture vessels at 20°C with no agitation overnight. Metamorphosed juveniles were carefully transferred using a trimmed transfer pipette to petri dishes with natural biofilm growth and the diatom *Nitzschia alba*. Water changes occurred daily for juveniles, and they were observed daily for changes in morphology and growth.

Observation and Live Imaging of Development

Embryonic sea urchin development was observed, and successive cell divisions were timed under temperature control at 20°C. Embryos were imaged from fertilization through the early pluteus stage on a Zeiss LSM 700 confocal microscope (Jena, Germany) with a 20x objective using differential interference contrast (DIC). Images were captured using the Zen software suite, and micrograph measurements were added using ImageJ (National Institutes of Health, Bethesda, MD, USA). Composite DIC images were rendered from z-stacks of animals at the 8-cell stage, at late gastrulation, and at the prism and pluteus stages using Helicon Focus Pro Unlimited (v6.8.0, Helicon Soft Ltd.). Upon reaching the pluteus stage, larvae were imaged daily and scored for the number of arms present, and the development of the coelomic structures. There is reduction in synchrony of development at the onset of feeding. Therefore, we defined a developmental milestone as a time range averaged across multiple batches of larvae, where >85% of individuals had progressed to a developmental stage defined by morphological features.

Images of the larvae were captured using a 10x objective on a Zeiss Stemi 2000-C microscope with an AxioCam ERc 5s. Z-stacks of all larval stages were focus stacked using Helicon Focus Pro Unlimited (v6.8.0, Helicon Soft Ltd.). Larval Stages IV-VI were tiled, as well as focus-stacked. Imaging of the progression of internal larval structures was taken on a Zeiss LSM 700 microscope using 20x 0.8 NA plan-apo objective with DIC optics. Juveniles were imaged live using a Leica M165F high magnification stereomicroscope with a Canon EOS 60D camera. A standard scale with 1 mm increments was used to measure post-metamorphic animals at each magnification imaged. The adult animals were imaged with a Canon EOS 60D camera. We focused our observations on cell populations of particular interest for developmental biologists including the small micromeres which later give rise to primordial germ cells[32,33,78,79], primary mesenchyme cells which contribute to skeletogenesis[35,36,80], and secondary mesenchyme cells[81] which later differentiate into immune cell populations as part of the larval and adult innate response[82,83].

ACKNOWLEDGEMENTS:

The authors thank Patrick Leahy for his suggestions on culturing optimization and larval rearing, and Andy Cameron for insight on staging of larvae. We would also like to thank Vic Vacquier and fellow members of the Hamdoun Lab for discussion of this manuscript. We gratefully acknowledge Kathy Le, and Kasey Mitchell for their assistance with larval care and animal husbandry throughout this study. This work was supported through a Diversity Supplement for KTN through NIH ES027921 as well as NIH ES030318 and the NSF 1840844 awarded to AH.

REFERENCES:

1. Seaver EC, Thamm K, Hill SD. Growth patterns during segmentation in the two polychaete annelids, Capitella sp. I and Hydroides elegans: comparisons at distinct life history stages. *Evolution & development*. 2005;7(4):312-326.
2. King N, Carroll SB. A receptor tyrosine kinase from choanoflagellates: molecular insights into early animal evolution. *Proceedings of the National Academy of Sciences*. 2001;98(26):15032-15037.
3. Martindale MQ, Pang K, Finnerty JR. Investigating the origins of triploblasty:mesodermal'gene expression in a diploblastic animal, the sea anemone Nematostella vectensis (phylum, Cnidaria; class, Anthozoa). *Development*. 2004;131(10):2463-2474.
4. Rawson PD, Burton RS. Functional coadaptation between cytochrome c and cytochrome c oxidase within allopatric populations of a marine copepod. *Proceedings of the National Academy of Sciences*. 2002;99(20):12955-12958.
5. Armbrust EV, Berges JA, Bowler C, et al. The genome of the diatom Thalassiosira pseudonana: ecology, evolution, and metabolism. *Science*. 2004;306(5693):79-86.
6. Foltz K, Hamdoun A. *Echinoderms*. Academic Press; 2019.
7. Hedgecock D, Lin J-Z, DeCola S, et al. Transcriptomic analysis of growth heterosis in larval Pacific oysters (Crassostrea gigas). *Proceedings of the National Academy of Sciences*. 2007;104(7):2313-2318.
8. Nichols SA, Dirks W, Pearse JS, King N. Early evolution of animal cell signaling and adhesion genes. *Proceedings of the National Academy of Sciences*. 2006;103(33):12451-12456.
9. Lemaire P. Evolutionary crossroads in developmental biology: the tunicates. *Development*. 2011;138(11):2143-2152.
10. Hodgkin AL, Huxley AF. Action potentials recorded from inside a nerve fibre. *Nature*. 1939;144(3651):710.
11. Skou JC. The influence of some cations on an adenosine triphosphatase from peripheral nerves. *Biochimica et biophysica acta*. 1957;23:394-401.
12. Chalfie M, Tu Y, Euskirchen G, Ward WW, Prasher DC. Green fluorescent protein as a marker for gene expression. *Science*. 1994;263(5148):802-805.
13. Heim R, Prasher DC, Tsien RY. Wavelength mutations and posttranslational autoxidation of green fluorescent protein. *Proceedings of the National Academy of Sciences*. 1994;91(26):12501-12504.
14. Metchnikoff E. *Untersuchungen über die intracelluläre Verdauung bei wirbellosen Thieren*. A. Hölder; 1883.
15. Evans T, Rosenthal ET, Youngblom J, Distel D, Hunt T. Cyclin: a protein specified by maternal mRNA in sea urchin eggs that is destroyed at each cleavage division. *Cell*. Jun 1983;33(2):389-96.
16. Hawkins RD, Abrams TW, Carew TJ, Kandel ER. A cellular mechanism of classical conditioning in Aplysia: activity-dependent amplification of presynaptic facilitation. *Science*. 1983;219(4583):400-405.

17. Shimomura O, Johnson FH, Saiga Y. Extraction, purification and properties of aequorin, a bioluminescent protein from the luminous hydromedusan, Aequorea. *Journal of cellular and comparative physiology*. 1962;59(3):223-239.
18. Sodergren E, Weinstock GM, Davidson EH, et al. The genome of the sea urchin Strongylocentrotus purpuratus. *Science*. 2006;314(5801):941-952.
19. Cary GA, Hinman VF. Echinoderm development and evolution in the post-genomic era. *Developmental biology*. 2017;427(2):203-211.
20. Leahy PS. Laboratory culture of Strongylocentrotus purpuratus adults, embryos, and larvae. *Methods in cell biology*. Vol 27. Elsevier; 1986:1-13.
21. Leahy PS, Cameron RA, Knox MA, Britten RJ, Davidson EH. Development of sibling inbred sea urchins: normal embryogenesis, but frequent postembryonic malformation, arrest and lethality. *Mechanisms of development*. 1994;45(3):255-268.
22. Hinegardner RT. Growth and development of the laboratory cultured sea urchin. *The Biological Bulletin*. 1969;137(3):465-475.
23. Hinegardner RT. Morphology and genetics of sea-urchin development. *American Zoologist*. 1975:679-689.
24. Zigler KS, Lessios HA. Speciation on the coasts of the new world: phylogeography and the evolution of bindin in the sea urchin genus Lytechinus. *Evolution*. 2004;58(6):1225-1241.
25. Wray GA. The evolution of larval morphology during the post-Paleozoic radiation of echinoids. *Paleobiology*. 1992;18(3):258-287.
26. Gonzalez P, Lessios HA. Evolution of sea urchin retroviral-like (SURL) elements: evidence from 40 echinoid species. *Molecular biology and evolution*. 1999;16(7):938-952.
27. Wray GA, Lowe CJ. Developmental regulatory genes and echinoderm evolution. *Systematic biology*. 2000;49(1):28-51.
28. Lawrence JM. *Edible sea urchins: biology and ecology*. Elsevier; 2006.
29. Cameron RA. Two species of Lytechinus (Toxopneustidae: Echinoidea: Echinodermata) are completely cross-fertile. *Bulletin of the Southern California Academy of Sciences*. 1984;83(3):154-157.
30. Schuel H. Secretory functions of egg cortical granules in fertilization and development: A critical review. *Gamete Research*. 1978;1(3-4):299-382.
31. Steinhardt RA, Epel D. Activation of sea-urchin eggs by a calcium ionophore. *Proc Natl Acad Sci U S A*. May 1974;71(5):1915-9. https://doi.org10.1073/pnas.71.5.1915.
32. Juliano CE, Voronina E, Stack C, Aldrich M, Cameron AR, Wessel GM. Germ line determinants are not localized early in sea urchin development, but do accumulate in the small micromere lineage. *Developmental biology*. 2006;300(1):406-415.
33. Campanale JP, Hamdoun A. Programmed reduction of ABC transporter activity in sea urchin germline progenitors. *Development*. 2012;139(4):783-792.
34. Itza EM, Mozingo NM. Septate junctions mediate the barrier to paracellular permeability in sea urchin embryos. *Zygote*. 2005;13(3):255-264.
35. Piacentino ML, Ramachandran J, Bradham CA. Late Alk4/5/7 signaling is required for anterior skeletal patterning in sea urchin embryos. *Development*. 2015;142(5):943-952.

36. Schatzberg D, Lawton M, Hadyniak SE, et al. H+/K+ ATPase activity is required for biomineralization in sea urchin embryos. *Developmental biology*. 2015;406(2):259-270.
37. Kimberly EL, Hardin J. Bottle cells are required for the initiation of primary invagination in the sea urchin embryo. *Developmental biology*. 1998;204(1):235-250.
38. Nakajima Y, Burke RD. The initial phase of gastrulation in sea urchins is accompanied by the formation of bottle cells. *Developmental biology*. 1996;179(2):436-446.
39. Ishizuka Y, Minokawa T, Amemiya S. Micromere descendants at the blastula stage are involved in normal archenteron formation in sea urchin embryos. *Development Genes & Evolution*. 2001;211(2).
40. Miller J, Fraser SE, McClay D. Dynamics of thin filopodia during sea urchin gastrulation. *Development*. 1995;121(8):2501-2511.
41. Annunziata R, Perillo M, Andrikou C, Cole AG, Martinez P, Arnone MI. Pattern and process during sea urchin gut morphogenesis: the regulatory landscape. *Genesis*. 2014;52(3):251-268.
42. Smith MM, Cruz Smith L, Cameron RA, Urry LA. The larval stages of the sea urchin, Strongylocentrotus purpuratus. *Journal of Morphology*. 2008;269(6):713-733.
43. Heyland A, Hodin J. A detailed staging scheme for late larval development in Strongylocentrotus purpuratus focused on readily-visible juvenile structures within the rudiment. *BMC developmental biology*. 2014;14(1):22.
44. Cameron RA, Hinegardner RT. Initiation of metamorphosis in laboratory cultured sea urchins. *The Biological Bulletin*. 1974;146(3):335-342.
45. Cameron RA, Hinegardner RT. Early events in sea urchin metamorphosis, description and analysis. *J Morphol*. Jul 1978;157(1):21-31. https://doi.org10.1002/jmor.1051570103.
46. Nieuwkoop PD. Normal table of Xenopus laevis (Daudin). *Normal table of Xenopus laevis (Daudin)*. 1956:162-203.
47. Nieuwkoop P, Faber J. Normal Table of Xenopus laevis (Daudin) Garland Publishing. *New York*. 1994;252.
48. Kakebeen A, Wills A. Advancing genetic and genomic technologies deepen the pool for discovery in Xenopus tropicalis. *Developmental Dynamics*. 2019;248(8):620-625.
49. Kimmel CB, Ballard WW, Kimmel SR, Ullmann B, Schilling TF. Stages of embryonic development of the zebrafish. *Developmental dynamics*. 1995;203(3):253-310.
50. Hamburger V, Hamilton HL. A series of normal stages in the development of the chick embryo. *Journal of morphology*. 1951;88(1):49-92.
51. Harvey EB. The growth and metamorphosis of the Arbacia punctulata pluteus, and late development of the white halves of centrifuged eggs. *The Biological Bulletin*. 1949;97(3):287-299.
52. MacBride EW. VI. The development of Echinus esculentus, together some points the development of E. miliaris and E. acutus. *Philosophical Transactions of the Royal Society of London Series B, Containing Papers of a Biological Character*. 1903;195(207-213):285-327.
53. Burke RD. The structure of the nervous system of the pluteus larva of Strongylocentrotus purpuratus. *Cell and tissue research*. 1978;191(2):233-247.
54. Burke RD. Development of pedicellariae in the pluteus larva of Lytechinus pictus (Echinodermata: Echinoidea). *Canadian Journal of Zoology*. 1980;58(9):1674-1682.

55. Burke RD. Morphogenesis of the digestive tract of the pluteus larva of Strongylocentrotus purpuratus: shaping and bending. *International Journal of Invertebrate Reproduction*. 1980;2(1):13-21.
56. Adams NL, Heyland A, Rice LL, Foltz KR. Procuring animals and culturing of eggs and embryos. *Methods in cell biology*. Vol 150. Elsevier; 2019:3-46.
57. Pawson DL, Miller J. Studies of genetically controlled phenotypic characters in laboratory-reared Lytechinus variegatus (Lamarck)(Echinodermata: Echinoidea) from Bermuda and Florida. Proceedings of the International Echinoderm Conference, Tampa Bay. AA Balkema, Rotterdam1982. p. 165-171.
58. Yaguchi S. Temnopleurus as an emerging echinoderm model. *Methods in cell biology*. Vol 150. Elsevier; 2019:71-79.
59. Croce J. *P. lividus* Stage Ontology. In: Nesbit KT, Hamdoun A, editors. Email thread of echinoderm staging and *P. lividus* development ed2019.
60. Steinhardt R. Intracellular free calcium and the first cell cycle of the sea-urchin embryo (Lytechinus pictus). *Journal of reproduction and fertility Supplement*. 1990;42:191.
61. Terasaki M, Jaffe LA. Organization of the sea urchin egg endoplasmic reticulum and its reorganization at fertilization. *J Cell Biol*. Sep 1991;114(5):929-40. https://doi.org10.1083/jcb.114.5.929.
62. Cserjesi P, Fairley P, Brandhorst BP. Functional analysis of the promoter of a sea urchin metallothionein gene. *Biochem Cell Biol*. Oct-Nov 1992;70(10-11):1142-50.
63. Cserjesi P, Fang H, Brandhorst BP. Metallothionein gene expression in embryos of the sea urchin Lytechinus pictus. *Molecular Reproduction and Development: Incorporating Gamete Research*. 1997;47(1):39-46.
64. Brandhorst BP. Two-dimensional gel patterns of protein synthesis before and after fertilization of sea urchin eggs. *Dev Biol*. Sep 1976;52(2):310-7.
65. Wu RS, Wilt FH. Poly A metabolism in sea urchin embryos. *Biochemical and biophysical research communications*. 1973;54(2):704-714.
66. Lee JJ, Calzone FJ, Britten RJ, Angerer RC, Davidson EH. Activation of sea urchin actin genes during embryogenesis: Measurement of transcript accumulation from five different genes in Strongylocentrotus purpuratus. *Journal of molecular biology*. 1986;188(2):173-183.
67. Nemer M, Infante AA. Messenger RNA in early sea-urchin embryos: size classes. *Science*. 1965;150(3693):217-221.
68. Poenie M, Alderton J, Tsien RY, Steinhardt RA. Changes of free calcium levels with stages of the cell division cycle. *Nature*. 1985;315(6015):147.
69. Lin C-Y, Su Y-H. Genome editing in sea urchin embryos by using a CRISPR/Cas9 system. *Developmental biology*. 2016;409(2):420-428.
70. Shevidi S, Uchida A, Schudrowitz N, Wessel GM, Yajima M. Single nucleotide editing without DNA cleavage using CRISPR/Cas9-deaminase in the sea urchin embryo. *Developmental Dynamics*. 2017;246(12):1036-1046.
71. Wessel GM, Kiyomoto M, Shen T-L, Yajima M. Genetic manipulation of the pigment pathway in a sea urchin reveals distinct lineage commitment prior to metamorphosis in the bilateral to radial body plan transition. *Scientific reports*. 2020;10(1):1-10.

72. Pickett C, Zeller RW. Efficient genome editing using CRISPR-Cas-mediated homology directed repair in the ascidian Ciona robusta. *genesis*. 2018;56(11-12):e23260.
73. Nakanishi N, Martindale MQ. CRISPR knockouts reveal an endogenous role for ancient neuropeptides in regulating developmental timing in a sea anemone. *Elife*. 2018;7:e39742.
74. Doudna JA, Charpentier E. The new frontier of genome engineering with CRISPR-Cas9. *Science*. 2014;346(6213):1258096.
75. Peng Y, Clark KJ, Campbell JM, Panetta MR, Guo Y, Ekker SC. Making designer mutants in model organisms. *Development*. 2014;141(21):4042-4054.
76. Hsu PD, Lander ES, Zhang F. Development and applications of CRISPR-Cas9 for genome engineering. *Cell*. 2014;157(6):1262-1278.
77. Nesbit KT, Fleming T, Batzel G, et al. The painted sea urchin, Lytechinus pictus, as a genetically-enabled developmental model. *Methods Cell Biol*. 2019;150:105-123. https://doi.org10.1016/bs.mcb.2018.11.010.
78. Pehrson JR, Cohen LH. The fate of the small micromeres in sea urchin development. *Developmental biology*. 1986;113(2):522-526.
79. Juliano CE, Swartz SZ, Wessel GM. A conserved germline multipotency program. *Development*. 2010;137(24):4113-4126.
80. Ettensohn CA. Cell interactions and mesodermal cell fates in the sea urchin embryo. *Development*. 1992;116(Supplement):43-51.
81. Tamboline CR, Burke RD. Secondary mesenchyme of the sea urchin embryo: ontogeny of blastocoelar cells. *Journal of Experimental Zoology*. 1992;262(1):51-60.
82. Smith LC, Rast JP, Brockton V, et al. The sea urchin immune system. *Invertebrate Survival Journal*. 2006;3(1):25-39.
83. Ho EC, Buckley KM, Schrankel CS, et al. Perturbation of gut bacteria induces a coordinated cellular immune response in the purple sea urchin larva. *Immunology and cell biology*. 2016;94(9):861-874.

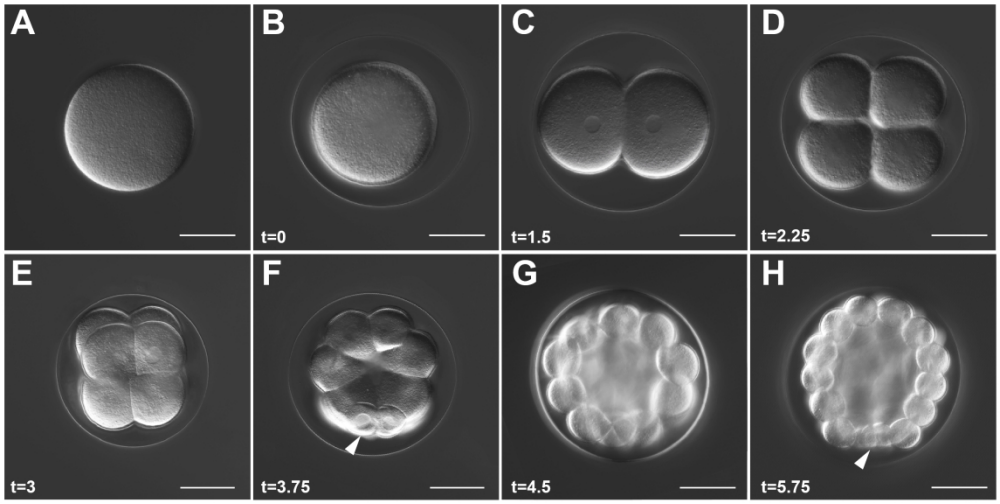

Figure 1. Early cleavages, A-V axis determination, and formation of the micromeres. A) Unfertilized egg. **B)** Zygote. **C)** 2-cell embryo. **D)** 4-cell embryo. **E)** 8-cell embryo. **F)** 16-cell embryo, white arrow points to the micromeres. **G)** 28-cell embryo. **H)** 60-cell embryo, white arrow points to the small micromeres. For all panels, scale = 50 μm. Time points listed in hours post-fertilization (hpf). All are oriented with the vegetal pole, where discernable (from the 16-60 cell stage), pointing down.

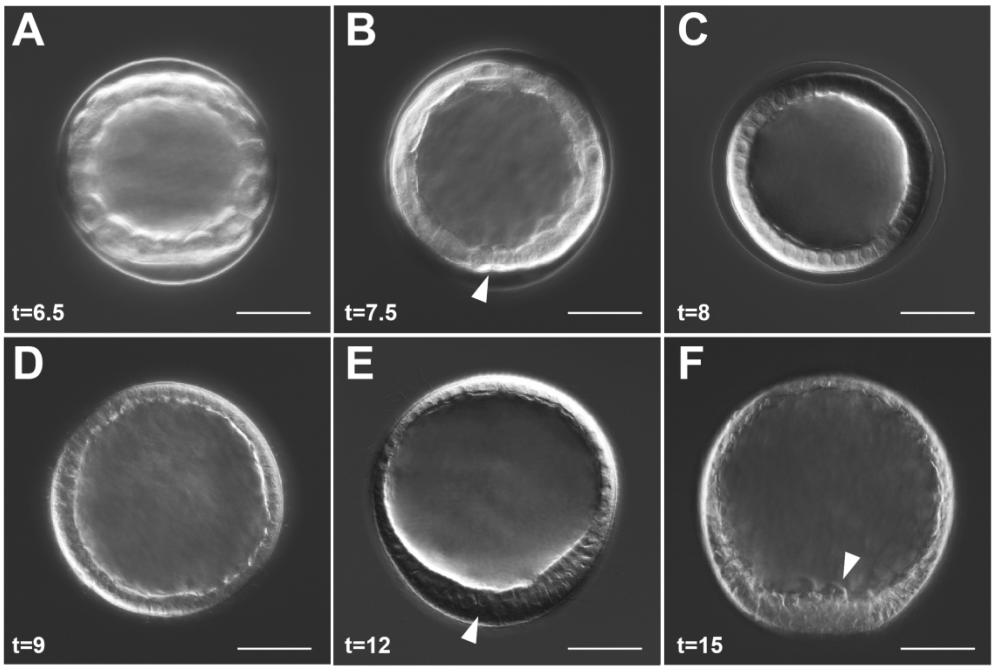

Figure 2. Blastula stages, hatching, and early ingression of PMCs in L. pictus. A) Early blastula stage. **B)** Embryos begin to demonstrate cell shape changes, and the small micromeres (white arrow) are visible at the vegetal pole. **C)** Blastula pre-hatching. **D)** Hatched blastula. **E)** White arrow points at the thickening at the vegetal plate. **F)** White arrow points at PMCs ingressing into the blastocoel, which are visible at the vegetal pole. For all panels, scale = 50 μm. Times listed in hours post-fertilization (hpf).

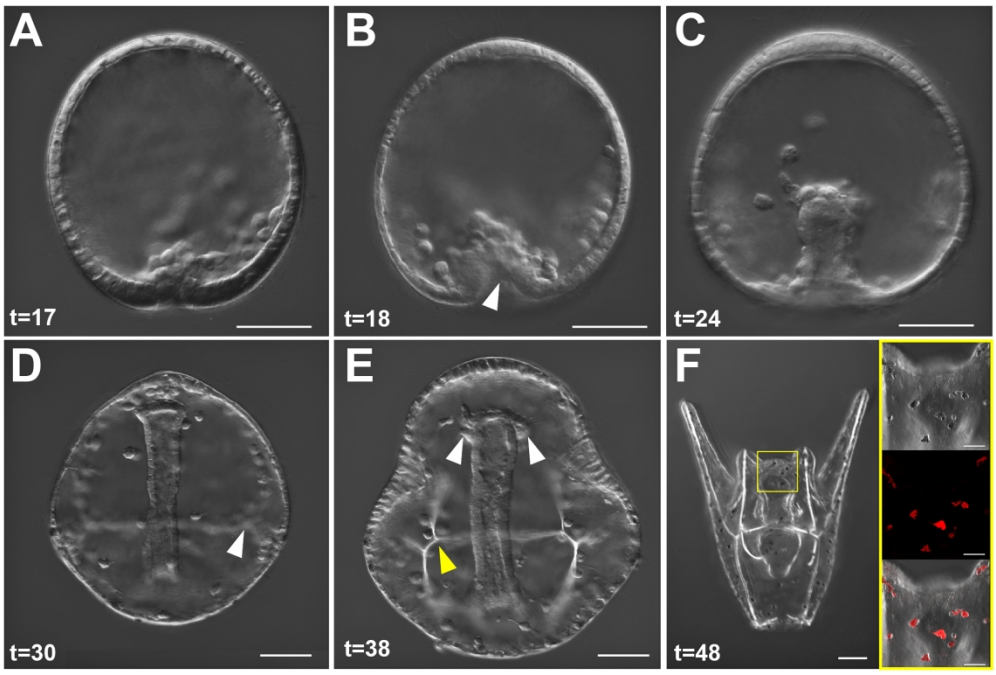

Figure 3. Gastrulation, SMC differentiation, and skeletal rod formation in L. pictus. A) First signs of invagination of the vegetal pole are apparent after ingression of PMCs. **B)** Primary gastrulation completes and the vegetal pole is turned inward as indicated by the white arrow. A population of SMCs ingress into the blastocoel and the PMCs begin to arrange around the developing archenteron. **C)** During mid-gastrulation the archenteron moves through the blastocoel and pigment cell precursors will migrate through the blastocoel to embed into the ectoderm during mid-late gastrulation. **D)** Late gastrulae have clear arrangement of PMCs and triradiate spicules which will further develop into the larval skeleton (white arrow). The archenteron has nearly reached the oral side of the animal. **E)** Evidence of the forming coelomic pouches (white arrows) on either side of the archenteron preclude the fusion of the mouth with the oral ectoderm during the prism larval stage, and the arms begin to bud out from the larval body as the skeletal supports (yellow arrow) are further elaborated. **F)** Composite stack of early pluteus larva in abanal view. The gut has differentiated into three parts. A yellow box surrounds the region of the larva shown in the inset. Inset shows DIC, fluorescence, and overlay of pigment cells which contain the autofluorescent pigment echinochrome A and are embedded into the ectoderm of the larva. For all panels, scale = 50 μm. Inset panels scale = 20 μm. Times listed in hours post-fertilization (hpf).

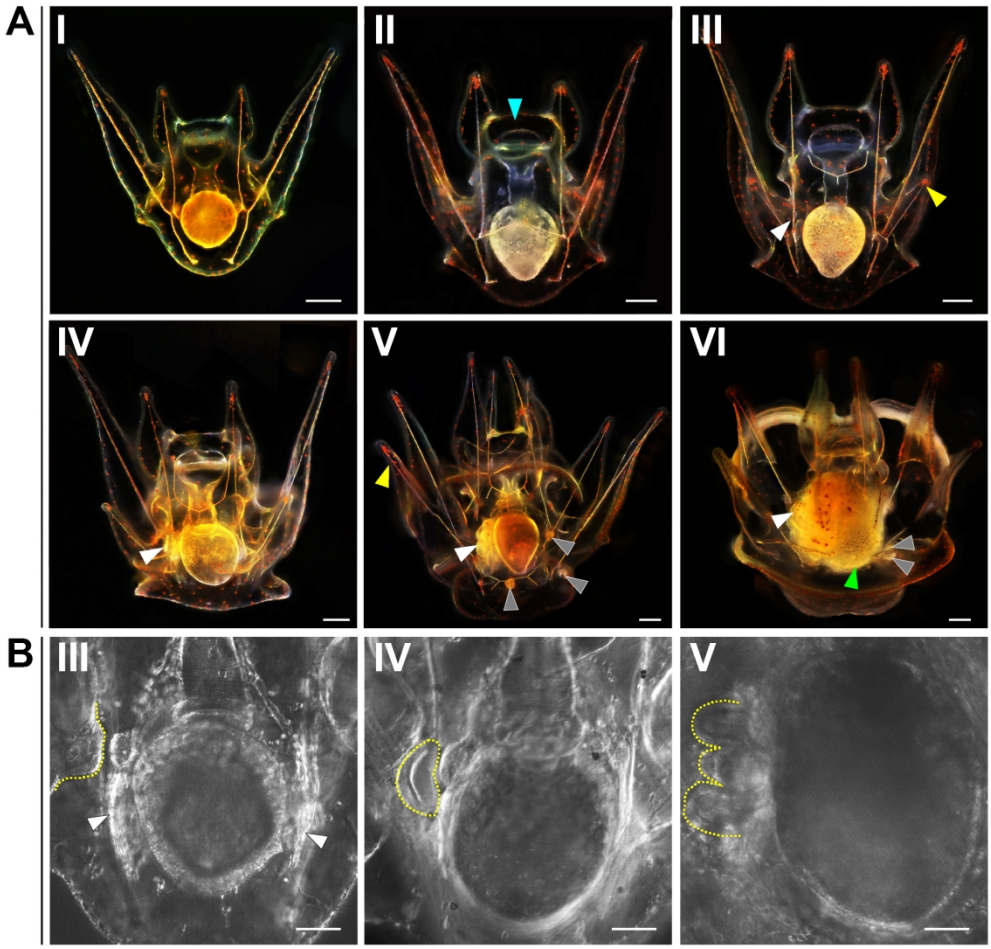

Figure 4. Larval staging of Lytechinus pictus. A) Scale = 250 microns. Stages I-VI of L. pictus. Blue arrow in 4A-II points to the oral hood tissue. White arrow in 4A-III marks the vestibular invagination. Yellow arrow in 4A-III marks the right posterodorsal arm. White arrow in 4A-IV marks the rudiment initiation adjacent to the gut. White arrow in 4A-V marks the pentagonal disc, while grey arrows denote the three pedicellariae, and the yellow arrow marks the fully formed left posterodorsal arm. White arrow in 4A-VI marks the fully formed rudiment, the green arrow marks the gut which now has a more textured appearance, and the grey arrows mark the two pedicellariae that are in view out of three. **B)** Scale = 50 microns. High magnification DIC imaging of the progression of development of coelomic structures during larval Stage III, IV, and V (from left to right). The dashed yellow lines highlight the vestibular invagination (left panel), the crescent-shaped initiation of the rudiment (middle), and the more elaborated organization of the rudiment tissues into the pentagonal disc (right panel).

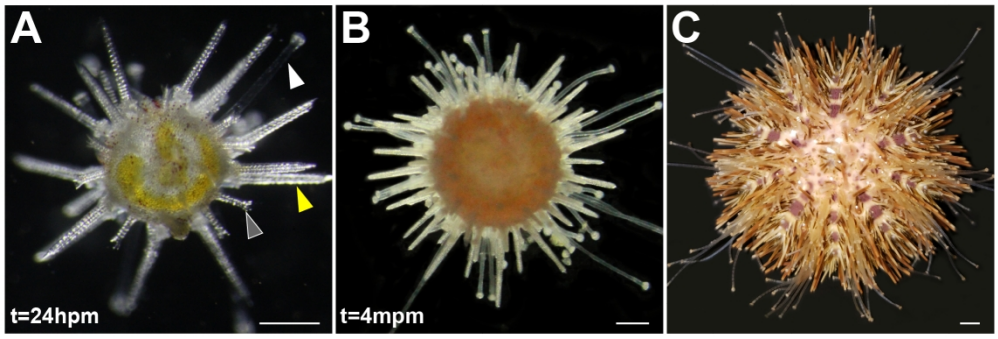

Figure 5. Post-metamorphic maturation of L. pictus. A) Juvenile at 24 hours post-metamorphosis (hpm). There are five tube feet (white arrow) as well as 20 walking spines (yellow arrow) and 10 juvenile spines (grey arrow). **B)** 4 months post-metamorphosis (mpm); **C)** Sexually mature adult. For all panels, scale = 0.5 mm.

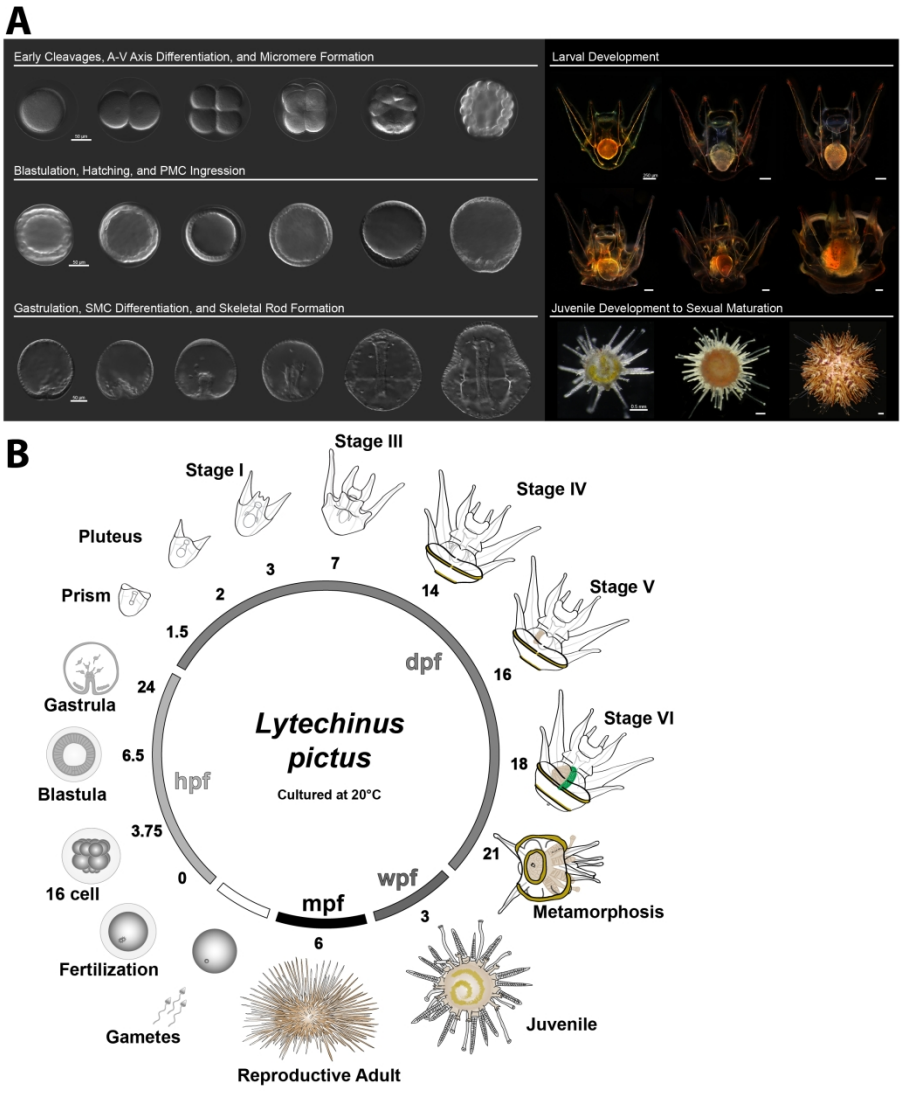

Figure 6. Summary of L. pictus development. A) Synopsis of major phases of development in the sea urchin L. pictus. **B)** Schematic of the L. pictus life cycle, illustrations are not to scale and time points are listed as the average time for >85% of individuals in a batch to reach a particular developmental stage.